Biochimica et Biophysica Acta 1847 (2015) 248–261

Contents lists available at ScienceDirect

Biochimica et Biophysica Acta

journal homepage: www.elsevier.com/locate/bbabio

Direct energy transfer from the major antenna to the photosystem II core complexes in the absence of minor antennae in liposomes

Ruixue Sun [a,b,1], Kun Liu [a,1], Lianqing Dong [a,b], Yuling Wu [a,b], Harald Paulsen [c], Chunhong Yang [a,*]

[a] Key Laboratory of Photobiology, Institute of Botany, Chinese Academy of Sciences, Nanxincun 20, Beijing 100093, China
[b] University of Chinese Academy of Sciences, Yuquan Road 19A, Beijing 100049, China
[c] Institut für Allgemeine Botanik, Johannes-Gutenberg-Universität Mainz, Johannes-von-Müllerweg 6, 55099 Mainz, Germany

ARTICLE INFO

Article history:
Received 9 May 2014
Received in revised form 13 November 2014
Accepted 18 November 2014
Available online 22 November 2014

Keywords:
Proteoliposome
Protein–protein interaction
Photosystem II
Light-harvesting complex
Minor antenna

ABSTRACT

Minor antennae of photosystem (PS) II, located between the PSII core complex and the major antenna (LHCII), are important components for the structural and functional integrity of PSII supercomplexes. In order to study the functional significance of minor antennae in the energetic coupling between LHCII and the PSII core, characteristics of PSII–LHCII proteoliposomes, with or without minor antennae, were investigated. Two types of PSII preparations containing different antenna compositions were isolated from pea: 1) the PSII preparation composed of the PSII core complex, all of the minor antennae, and a small amount of major antennae (MCC); and 2) the purified PSII dimeric core complexes without periphery antenna (CC). They were incorporated, together with LHCII, into liposomes composed of thylakoid membrane lipids. The spectroscopic and functional characteristics were measured. 77 K fluorescence emission spectra revealed an increased spectral weight of fluorescence from PSII reaction center in the CC–LHCII proteoliposomes, implying energetic coupling between LHCII and CC in the proteoliposomes lacking minor antennae. This result was further confirmed by chlorophyll *a* fluorescence induction kinetics. The incorporation of LHCII together with CC markedly increased the antenna cross-section of the PSII core complex. The 2,6-dichlorophenolindophenol photoreduction measurement implied that the lack of minor antennae in PSII supercomplexes did not block the energy transfer from LHCII to the PSII core complex. In conclusion, it is possible, in liposomes, that LHCII transfer energy directly to the PSII core complex, in the absence of minor antennae.

1. Introduction

Photosystem (PS) II is a multisubunit pigment–protein complex that utilizes the solar energy to catalyze water splitting and plastoquinone reduction in the thylakoid membrane of cyanobacteria, algae and higher plants. It supplies oxygen and energy for life on earth and is therefore called "the engine of life" [1]. The subunits of PSII can be classified into two groups: the PSII core complex and the peripheral antenna system. The PSII core complex mainly consists of three structural domains: the PSII reaction center (RC) composed of D1 and D2 proteins that stabilize the carriers for charge separation and primary electron transport, the inner antennae CP47 and CP43, and a set of extrinsic proteins on the lumen side involved in oxygen evolution. There are also several other low molecular subunits in the core complex [2]. Detailed structural information on the PSII core complex of cyanobacteria was obtained from high resolution X-ray diffraction [3–8]. The PSII core complex of higher plants has been studied at lower resolution by electron crystallography [9–11].

The peripheral antenna system of PSII is responsible for light harvesting, for energy transfer to PSII RC, for dissipating excess energy as heat, and for regulating the distribution of excitation energy between PSI and PSII [12]. In higher plants, the major antenna of PSII (the light-

Abbreviations: Chl, chlorophyll; DCMU, 3-(3,4-Dichlorophenyl)-1,1-dimethylurea; DCPIP, 2,6-Dichlorophenol indophenol; β-DDM, dodecyl-β-D-maltoside; DGDG, digalactosyl diacylglycerol; DPC, 1,5-Diphenylcarbazide; LHCII, major antenna of photosystem II; MGDG, monogalactosyl diacylglycerol; TLC, thin-layer chromatography; NPQ, non-photochemical quenching; OEC, oxygen evolution complex; OG, n-octyl-β-D-glucopyranoside; PG, phosphatidylglycerol; PL, proteoliposomes; PS, photosystem; RC, reaction center; SQDG, sulfoquinovosyl diacylglycerol; MCC, PSII preparation with PSII core complex, minor antennae, and small amounts of major antennae; CC, purified PSII core complex without peripheral antenna; MCC PL, MCC proteoliposomes; CC PL, CC proteoliposomes; LHCII PL, LHCII proteoliposomes; L2MCC PL, MCC–LHCII proteoliposomes co-inserted with 2 mol LHCII trimers per PSII RC dimer; L2CC PL, CC–LHCII proteoliposomes co-inserted with 2 mol LHCII trimers per PSII RC dimer; L6MCC PL, MCC–LHCII proteoliposomes co-inserted with 6 mol LHCII trimers per PSII RC dimer; L6CC PL, CC–LHCII proteoliposomes co-inserted with 6 mol LHCII per PSII RC dimer; MCC PL + L2 PL, mixture of MCC PL and LHCII PL with the same LHCII/PSII RC ratio as L2MCC PL; CC PL + L2 PL, mixture of CC PL and LHCII PL with the same LHCII/PSII RC ratio as L2CC PL; MCC PL + L6 PL, mixture of MCC PL and LHCII PL with the same LHCII/PSII RC ratio as L6MCC PL; CC PL + L6 PL, mixture of CC PL and LHCII PL with the same LHCII/PSII RC ratio as L6CC PL

* Corresponding author. Tel.: +86 1062836252; fax: +86 1062836219.
E-mail address: yangch@ibcas.ac.cn (C. Yang).

[1] The two authors contributed equally to this work.

http://dx.doi.org/10.1016/j.bbabio.2014.11.005
0005-2728/

harvesting complexes of PSII, LHCII), composed of the nuclear-encoded proteins Lhcb1-3, also play important roles in lateral segregation of the main pigment-protein complexes in thylakoid membrane and maintaining the grana structure [13]. Three minor antennae, CP29, CP26 and CP24, the products of Lhcb4-6 genes, are present as monomers in vivo. The antenna system of PSII is highly dynamic, undergoing flexible changes in coping with the changing environments [14]. Electron microscopic analyses show that the PSII–LHCII supercomplexes are composed of several LHCII trimers associated with the PSII core complex, with minor antennae located between them [15–18]. Normally, two strongly bound LHCII trimers (S-LHCII, S_2) and two moderately bound LHCII trimers (M-LHCII, M_2) are associated with dimeric PSII core complex to form $C_2S_2M_2$ supercomplexes. This is proposed to represent the general organization of PSII–LHCII supercomplexes and to act as the structural and functional basic unit for PSII [19,20]. In addition, there are also abundant "extra" LHCII trimers [21].

Studies on the functions of minor antennae have mainly been focused on three aspects: 1) the assembly of PSII supercomplexes; 2) energy transfer from LHCII to the PSII core complex and 3) photoprotection or photoinhibition. It is reported that CP29 plays a crucial role in the assembly and stability of the supercomplexes since no PSII–LHCII supercomplex could be found upon mild detergent solubilization of thylakoid membrane from plants lacking CP29 [22]. Nevertheless, de Bianchi et al. [23] presented the evidence that it was still possible to form C_2S_2M and $C_2S_2M_2$ particles without CP29 in the *koLhcb4* mutant. Functionally, an *Arabidopsis thaliana* mutant lacking CP29 showed decreased maximal photosynthetic efficiency of PSII and reduced capacity for non-photochemical quenching (NPQ) [23,24]. Recently, a possible path for NPQ in CP29 was assigned based on its high-resolution crystal structural analysis [25]. Picosecond fluorescence kinetics measurement revealed that lack of CP29 decreased the energy migration kinetics from LHCII to PSII RC [26]. Conflicting observations have been presented regarding the structural significance of CP24. In *A. thaliana*, it is reported to be necessary for the association of the M-LHCII to the PSII core and the electron transport in the thylakoid membrane [27,28], While in *Chlamydomonas reinhardtii*, each dimeric PSII core can still bind up to six LHCII trimers in the absence of CP24 [29]. Furthermore, it has been observed that the energy migration kinetics from LHCII to the PSII core is slowed down in thylakoids lacking CP24 [26]. In contrast to CP24 and CP29, CP26 seems to be neither important in the assembly of PSII supercomplexes, nor have any effect on the energy migration in PSII [22,26,27,30]. Furthermore, CP26 can adopt a trimeric structure and function as major antenna in case Lhcb1-2 are lacking [31]. The picosecond-fluorescence spectroscopy measurement showed that the migration time from LHCII to the PSII core increased enormously in the thylakoid membrane of the *A. thaliana* line depleted of all the minor antennae [32].

The photosynthetic membrane is a complex biological membrane system containing densely packed proteins in a lipid bilayer, about half of which consists of non-bilayer lipids. The lipids not only function as a matrix stabilizing different photosynthetic pigment–protein supercomplexes, but also influence the structure and function of the proteins via specific or non-specific interactions with the membrane proteins [33,34]. As a complement to in vivo studies, the incorporation of membrane proteins into artificial membranes has become an important tool for evaluating the functions of membrane proteins and their interactions with one another and with lipids [35]. It is based on pioneering work with liposomes composed of different lipids which showed that different photosynthetic membrane proteins could be incorporated and interact with one another in liposome membranes [36–39].

The technique has been used in this work for studying functions of all the minor antennae as a complete set. Two types of PSII preparations with different antennae compositions were isolated from pea and co-reconstituted with LHCII into liposomes composed of thylakoid membrane lipids. The spectroscopic and functional characteristics of different PSII–LHCII proteoliposomes were compared to mixtures of liposomes containing only PSII preparations with liposomes containing LHCII, but of similar net composition. The results show that in this in vitro system, energy transfer is possible from LHCII to PSII RC in the absence of any minor antennae.

2. Materials and methods

2.1. Isolation of PSII complexes and LHCII

Pea (*Pisum sativum* L.) was grown in a 14-h photoperiod under an irradiance of 100 μmol photons/m^2/s. The temperature and relative humidity were set at 23/19 °C (day/night) and 70%, respectively. BBY membranes were isolated from 2-week-old pea leaves according to Berthold et al. [40] with proper modifications due to the characteristic compositions of pea thylakoid in contrast to spinach. The whole isolation process was performed on ice in a dark room under a 520 nm LED illumination. The BBY membrane with chlorophyll (Chl) concentration of 2 mg/mL was resuspended in the storing buffer (15 mM NaCl, 5 mM $CaCl_2$, 0.5 M betaine, 0.4 M sucrose, 20 mM MES–NaOH, pH 6.5), then frozen in liquid nitrogen and stored at −80 °C. The Chl concentration was determined according to Porra et al. [41].

PSII preparations (MCC) composed of PSII core, all the minor antennae, and a small amount of major antennae were purified according to the modified method of Hankamer et al. [42]. Frozen BBY membrane containing 120 mg Chl was slowly thawed on ice and dispersed in 180 mL buffer A (0.5 M sucrose, 40 mM MES NaOH, pH 6.0) and centrifuged for 15 min at 48,000 ×*g*. The pellet was resuspended in 24 mL buffer B (1.8 M sucrose, 18 mM NaCl, 72 mM $MgCl_2$, 72 mM MES–NaOH, pH 6.0) and centrifugation tubes were quickly rinsed with 17 mL 346 mM n-octyl-β-D-glucopyranoside (OG) (Merck, Germany). The suspension was homogenized and incubated, under stirring, on ice for 75 min. Then 70 mL buffer A was added into the suspension and the mixture was centrifuged for 10 min at 48,000 ×*g*. The supernatant was combined with 195 mL buffer C (40 mM MES–NaOH, pH 6.0) and centrifuged for 1 h at 150,000 ×*g*. The supernatant was diluted by a half volume of buffer C and then centrifuged for 30 min at 50,000 ×*g*. The pellet was resuspended in a small volume of liposome buffer (10 mM NaCl, 25 mM MES–NaOH, pH 6.5) and homogenized in a glass homogenizer. MCC with a final Chl concentration of 1 mg/mL was frozen in liquid nitrogen and stored at −80 °C.

Purified PSII core complexes (CC) were isolated starting from MCC according to Hankamer et al. [42] with some modifications. The MCC was incubated with 25 mM dodecyl-β-D-maltoside (β-DDM) (Anatrace, Inc., UK) with stirring for 10 min on ice. The suspension was layered on the top of a continuous sucrose density gradient (0.5 M sucrose, 0.03% (w/v) β-DDM, 10 mM NaCl, 5 mM $CaCl_2$, 25 mM MES–NaOH, pH 6.5) formed by freeze–thaw method and centrifuged at 90,000 ×*g* for 5 h in a VTi 50 rotor (Beckman Coulter, Inc., USA). The band corresponding to dimeric PSII core complex was collected and then concentrated at 5000 ×*g* for 30 min with an Amicon Ultra®-15 membrane filter with a 100 kDa cutoff (Millipore, USA). CC was immediately adjusted to proper Chl concentration and used for assays.

Large amounts of crude LHCII were prepared from pea by the method described in Rühle and Paulsen [43]. The crude LHCII was further purified to avoid the contamination from minor antennae according to Liu et al.. The crude LHCII was solubilized completely with 1% (w/v) OG at a Chl concentration of 4 mg/mL and subjected to gel-filtration chromatography using a Superdex® 200 Hiload® 16/600 column (General Electric Company, USA) in an ÄKTA® Purifier system (General Electric Company, USA) [44]. The fractions of LHCII trimers were collected and precipitated with 100 mM KCl. After it was rinsed twice using distilled water, LHCII was frozen in liquid nitrogen and stored at −80 °C.

2.2. Reconstitution of the PSII core complexes and LHCII into liposomes

The four thylakoid membrane lipids (Lipid Products, Ltd., UK) were mixed at the ratio: monogalactosyl diacylglycerol (MGDG)/digalactosyl diacylglycerol (DGDG)/phosphatidylglycerol (PG)/sulfoquinovosyl diacylglycerol (SQDG) of 50/30/12/8 (w/w/w/w). An aliquot of a mixture containing 15 mg lipids was evaporated to form a thin film on the inner wall of a round-bottom flask. The lipid film was hydrated in liposome buffer by 30 s intermittent vibration every 5 min for 1 h at 40 °C [45]. The lipid suspension, with the final lipid concentration of 5 mg/mL, was passed through a polycarbonate membrane with a pore size of 0.2 μm in a Mini-Extruder (Avanti Polar Lipids, Inc., USA). Suspensions of PSII preparations and LHCII were sonicated for 1 min in a bath sonicator at 4 °C and then the PSII preparations were reconstituted individually or together with LHCII into the liposomes at the lipid/protein ratio of 4/1 (w/w), and correspondingly, the molar Chl/lipid ratios for LHCII, MCC and CC proteoliposomes to 1/9, 1/20 and 1/25, respectively. The ratio of LHCII/PSII for the co-reconstitution was set so that each PSII RC dimer in MCC or CC corresponded to two or six LHCII trimers. The reconstitution was induced by incubation with 0.1% (w/v) dodecyl-α-D-maltoside (Anatrace, Inc., UK) for 30 min at room temperature. The detergent was removed by an overnight incubation with degassed Bio-beads® SM-2 (Bio-Rad Laboratories, Inc., USA) at 4 °C.

2.3. Electrophoresis and Western blot analysis

The procedure of Tricine-SDS-PAGE was carried out according to Schägger [46]. The samples were loaded on the equal Chl basis. The samples were mixed with a loading buffer (12% (w/v) SDS, 6% (v/v) β-mercaptoethanol, 30% (w/v) glycerol, 0.05% (w/v) Coomassie Brilliant Blue G-250, 150 mM Tris–HCl, pH 7.0). The samples containing PSII RC were incubated for 30 min at 40 °C and the LHCII sample was boiled for 5 min before loading to the gels.

For immunoblotting analysis, proteins after Tricine-SDS-PAGE electrophoresis were electrophoretically transferred to a nitrocellulose membrane (General Electric Company, USA) and then probed with antibodies against Lhcb1, Lhcb2, Lhcb3, CP29, CP26, CP24 and CP47 (Agrisera, Sweden) according to standard procedures. The DyLight™ 800 labeled secondary antibody (Kirkegaard & Perry Laboratories, Inc., USA) was detected by scanning for infrared signal using the Odyssey Infrared Imaging System (LI-COR Biosciences, Inc., USA).

2.4. Freeze-fracture and transmission electron microscopy

For freeze-fracture electron microscopy, the proteoliposomes were frozen by jet freezing methods [47]. The replicas of freeze-fractured samples were made using a Balzers® BAF400 freeze-etch apparatus equipped with a rotating-cold stage. The replicas were floated onto 300 mesh copper grids. All specimens were examined in a 6750 TEM (Hitachi Ltd., Japan) equipped with a Gatan® 830 CCD camera.

2.5. Nycodenz density gradient flotation of proteoliposomes

A 10% to 40% (w/v) linear Nycodenz (Axis-Shield PoC AS, Norway) gradient in liposome buffer was made with the Gradient Master (BioComp Instruments, Inc., Canada). Reconstituted proteoliposomes in 7.5% (w/v) Nycodenz were layered onto the top of gradient and then centrifuged for 3 h at 300,000 ×*g* at 4 °C (SW55 rotor, Beckman). For further lipids and protein composition analyses, the green bands corresponding to the proteoliposomes were collected from Nycodenz density gradient and then concentrated with Amicon® Ultra-2 membrane filters with a 3 kDa cutoff (Millipore, USA) and resuspended again in the liposome buffer.

2.6. Thin-layer chromatography (TLC)

Total lipids in the proteoliposomes, collected from Nycodenz density gradient after the ultracentrifugation, were extracted with the method described by Sato and Tsuzuki [48]. Extracts were dried, and then solubilized in chloroform/methanol (2/1, v/v). The lipids were separated by thin-layer chromatography on 20 cm × 20 cm aluminum-backed silica gel plates (Merck, Germany). A lipid mixture containing four isolated thylakoid lipids at the ratio similar to thylakoid membrane (MGDG/DGDG/SQDG/PG = 50/30/12/8, w/w/w/w) were used as the reference for the samples. The exact volume of the lipid extracts was spotted at the starting point, and the TLC was developed in chloroform/methanol/25–28% ammonia solution (65/30/4, v/v/v). The TLC plate is sprayed with 0.01% (w/v) primulin (in 80% acetone) and visualized by exposure to 365 nm UV light.

2.7. Chemical cross-linking and in-gel digestion

A water-soluble cross-linkers reagent (ethylene glycol bis(succinimidyl succinate), Sulfo-EGS, Thermo Fisher Scientific) with a spacer length of 16.1 Å, that can react with the primary amino groups was used for cross-linking reaction. The experiment was carried out according to the manufacturer's manual. The proteoliposomes collected from the Nycodenz gradient were adjusted to a final Chl concentration of 0.2 mg/mL in a reaction buffer containing 5 mM NaCl and 50 mM HEPES (pH 7.5). The chemical cross-linking reaction was carried out with 10 mM Sulfo-EGS in dark at room temperature for 30 min and was quenched with 45 mM Tris–HCl (pH 7.5) at room temperature for 15 min.

Cross-linked proteins corresponding to 2 μg Chl were separated with Tricine-SDS-PAGE. Gel slices from 25 kDa to 100 kDa were cut and underwent trypsin digestion (Trypsin Gold, mass spectrometry grade, Promega) according to Shevchenko et al. [49].

2.8. Liquid chromatography/tandem mass spectrometry (LC–MS/MS) analysis and database search

Peptide aliquots (~200 ng) were analyzed in the Q Exactive (Thermo Fisher Scientific) mass spectrometer coupled to an UltiMate 3000 (Thermo Fisher Scientific Dionex) liquid chromatography system. The mobile phase consisted of Buffer A (formic acid–water, 0.1%, v/v) and Buffer B (formic acid–acetonitrile, 0.1%, v/v). The peptides were separated with an analytical column (Venusil XBP, C18(L), 5 μm, pore size: 150 Å, Bonna-Agela Technologies), ramping at a 90-min linear gradient from 5% to 35% buffer B at rate of 300 nL/min. The eluted sample was directly introduced onto the mass spectrometer.

MS were acquired over *m/z* 350–2000 at a resolution of 35,000. Precursors of +1 and +2 were excluded and data-dependent acquisition selected the top 15 most abundant precursor ions for tandem mass spectrometry by HCD fragmentation using an isolation window of *m/z* 2.0, collision energy of 32, and a resolution of 17,500. Monoisotopic screening was enabled and a dynamic exclusion window was set to 15.0 s.

LC–MS/MS data in Thermo Xcalibur.raw files were converted into .mgf format by Proteome Discoverer 1.3 (Thermo Fisher Scientific). A protein database containing 21 PSII subunits and 3 LHCII was established from the subprotein database for *P. sativum* of GenBank. For cross-link peptide search in MassMatrix [50], each protein sequence in the custom database was paired. The MassMatrix search parameters were set as follows: fixed modification: none; variable modification: oxidation of M, oxidation of HW, pyro-glu from QE, methylation of K, R, and N-term, and amidation of C-term, max # variable PTM/ peptide: 2; peptide tolerance: 6 ppm, MS/MS tolerance: 0.03 Da, mass type: monoisotopic, C13 isotope ions: Yes; enzyme: trypsin, missed cleavages: 2, peptide length: from 4 to 40; cross-link search mode: exploratory, and cross-link sites cleavability: non-cleavable by enzyme, and max

cross-links/peptide: 2. If the inter-peptides cross-link candidate's score was significant according to MassMatrix's algorithms, it was further manually validated based on the crystal structure of PSII from *Thermosynechococcus vulcanus* (PDB ID 3ARC) [3] and LHCII from *P. sativum* (PDB ID 2BHW) [13] and interpretation of product ion spectra. The confirmed results were annotated using pLabel [51].

2.9. Absorption and 77 K fluorescence spectrum measurements

Absorption spectra were recorded at room temperature with a UV–Vis 4550 spectrophotometer (Shimadzu Corporation, Japan) by using 1 cm path length cuvettes. 77 K fluorescence spectra were recorded with an F-7500 fluorescence spectrophotometer (Hitachi, Ltd., Japan) upon 436 nm or 480 nm excitations. The samples were diluted with liposome buffer to a Chl concentration of 10 μg/mL or 1.5 μg/mL for absorption spectra or for 77 K fluorescence spectra measurements, respectively.

2.10. Photochemical activity assays

Oxygen evolution activity of PSII proteoliposomes was measured with a Clark-type electrode system (Hansatech Instruments, Ltd., UK) at 25 °C. The Chl concentration of samples were adjusted to 10 μg/mL with oxygen evolution buffer (300 mM sucrose, 10 mM NaCl, 5 mM $CaCl_2$ and 25 mM MES–NaOH, pH 6.5) with 0.5 mM 2,5-dichloro-*p*-benzoquinone as electron acceptors. The photon flux density of the white light was 1200 μmol photons/m^2/s or 3900 μmol photons/m^2/s.

The photoreduction rate of 2,6-dichlorophenolindophenol (DCPIP) of PSII proteoliposomes was measured in the presence of an artificial electron donor 1,5-diphenylcarbazide (DPC). The photoreduction was induced by either white light (tungsten halogen lamp) or blue light (CREE® XLamp XP-E 465–485 nm LED, through 480 ± 2 nm narrow bandpass filter) at the light intensity of 300 μmol photons/m^2/s for 2 min. MCC-containing proteoliposomes and CC-containing proteoliposomes at Chl concentrations of 5 μg/mL and 2 μg/mL, respectively, were incubated in liposome buffer containing 75 μM DCPIP and 0.5 mM DPC. An extinction coefficient for DCPIP of 12.5/mM/cm (25 °C, pH 6.5) was used for the rate calculations.

2.11. Chlorophyll a fluorescence induction kinetics assay

Dark-adapted proteoliposomes were diluted with liposome buffer to a Chl concentration of 10 μg/mL. Chl *a* fluorescence induction curves were measured with Hansatech Handy-PEA (Hansatech Instruments, Ltd., UK), with the incident light passed through a glass filter producing a light spectrum from 380 to 580 nm. Chl *a* fluorescence induction curves were measured in the presence of 1 mM NH_2OH and 75 μM 3-(3,4-dichlorophenyl)-1,1-dimethylurea (DCMU) under irradiation of 600 μmol photons/m^2/s.

3. Results

3.1. Purification and characterization of different PSII pigment–protein complexes

In order to obtain PSII proteoliposomes with or without minor antennae, two types of PSII complexes were prepared. The first one including both the PSII core complexes and the minor antennae was termed MCC (PSII core complexes with minor antennae). The other including only the PSII core complexes without minor antennae was termed CC (PSII core complexes). BBY particles were also prepared for the control experiments. Fig. 1 shows the Tricine-SDS-PAGE profiles and Western blot analysis based on the same Chl loading, with series of dilutions, and the spectroscopic characterization of these PSII preparations. Because the CC sample contained very little Chl, the lane with 100% loading was severely overloaded, which is still shown so that the possible small amount of antenna protein contamination could be detected. Tricine-SDS-PAGE was also run based on the same PSII RC (CP47 as the standard) loading (Fig. S1), so that the amount of antennae per PSII RC could be evaluated. MCC and BBY preparations contain almost the same protein subunits, except that there was a much lower amount of LHCII subunits per PSII RC (CP47) in the MCC than that in the BBY membrane (Fig. 1A and Fig. S1). CC was mainly composed of the D1/D2/Cyt b559, the two inner antennae complexes CP47 and CP43. There was no trace of major antenna protein in the CC detected by immunoblotting based on the same Chl loading (Fig. 1B). It can also be seen from Fig. 1B that the CC was free of almost all the minor antenna except Lhcb5. There is a faint Lhcb5 signal in the lane with a very high protein loading (Fig. 1B). The amount of Lhcb5 in the CC was quantified. For this purpose, immunoblotting analysis to various amounts of BBY (corresponding to 0.2, 0.6, 0.8, 1.0, 1.2, 1.4 and 1.6 μg Chls) was executed so as to get calibration curves for CP47 and Lhcb5, respectively (data not shown). The relationship between the signals of CP47 and Lhcb5 in BBY was calculated. Based on this experiment, the relative amount of Lhcb5/CP47 in CC was calculated, which turned out that CC contained only 0.83% ± 0.11% (n = 5) Lhcb5 (CP26) per CP47 of that in the BBY preparation. Assuming that the Lhcb5/PSII RC (CP47) in BBY is 1, the ratio of Lhcb5/PSII RC in the CC preparation was only 0.0083.

The activities of these PSII preparations were assessed by their oxygen evolution rates (Table 1), measured at light intensities of 1200 or 3900 μmol photons/m^2/s, which were the under-saturating light intensity and saturating light intensity, respectively (Fig. S2). At 1200 μmol photons/m^2/s, the BBY preparation showed an oxygen evolution rate of 324.7 ± 4.1 μmol O_2/mg Chl/h. MCC gave an oxygen evolution rate of 329.5 ± 12.9 μmol O_2/mg Chl/h, whereas CC reached values of 613.4 ± 13.4 μmol O_2/mg Chl/h. At saturating light intensity (3900 μmol photons/m^2/s), the oxygen evolution rates of BBY, MCC and CC were increased to 537.8 ± 17.3 O_2/mg Chl/h, 527.2 ± 24.5 O_2/mg Chl/h and 1387.2 ± 38.3 O_2/mg Chl/h, respectively.

Fig. 1C shows the absorption spectra, normalized to the absorption maxima of Chl *a* at the Q_y region, of the three PSII preparations and LHCII, all dissolved in 0.1% (w/v) β-DDM. The absorption of Chl *a* of all the PSII preparations showed two main peaks around 435 nm and 675 nm. The absorption maxima of Chl *b* were around 470 nm and 650 nm. As expected, LHCII, with a Chl *a*/*b* ratio of 1.3, had the highest Chl *b* peaks, followed by the BBY membrane with a Chl *a*/*b* ratio of 2.0, and then the MCC with a Chl *a*/*b* ratio of 4.2. CC, whose Chl *a*/*b* ratio was 38.4, showed almost no Chl *b* absorption, which indicated that virtually all the Chl *b* had been removed from the purified CC.

The 77 K fluorescence emission spectra of the different PSII preparations and LHCII are presented in Fig. 1D. LHCII showed a single maximum at 679 nm, which is the typical Chl *a* fluorescence of trimeric LHCII [52]. BBY displayed a wide fluorescence emission spectrum peaking at 683.4 nm. Both types of PSII core preparations showed the maximal fluorescence emissions around 685 nm, which is typical for PSII RC [53]. They peaked at 684.6 and 685.6 nm for MCC and CC, respectively.

3.2. Incorporation of PSII preparations into liposomes

MCC or CC was either reconstituted individually or together with LHCII into liposomes made of thylakoid lipids. The proteoliposomes containing only the major antenna, LHCII, were named LHCII PL, and those containing only MCC or CC were named MCC PL or CC PL, respectively. The proteoliposomes co-inserted with MCC or CC together with different amounts of major antenna corresponding to 2 or 6 mol of LHCII trimers per PSII RC dimer were named L2MCC PL and L2CC PL or L6MCC PL and L6CC PL, respectively. The mixtures of LHCII PL with the ones containing only PSII core preparations (MCC PL or CC PL) were named MCC PL + LHCII PL or CC PL + LHCII PL, respectively. They contained the same amount of pigments and at the same LHCII/PSII RC

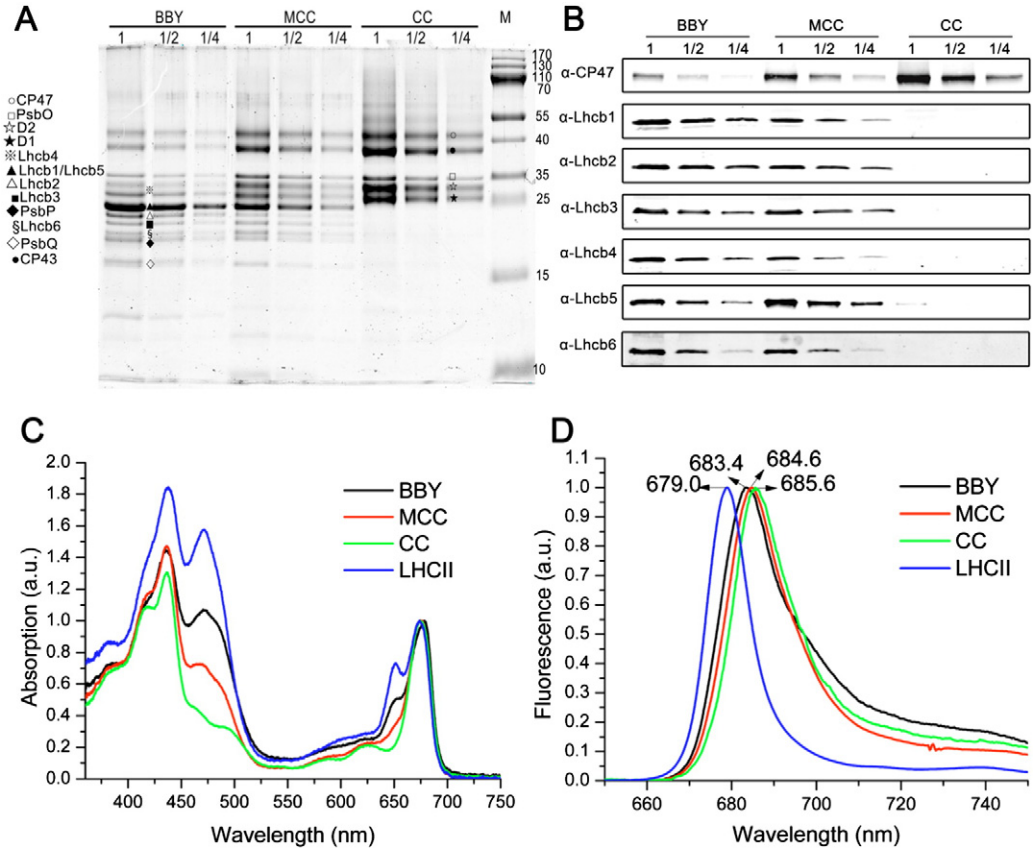

Fig. 1. Characteristics of different PSII preparations and LHCII. (A) Tricine-SDS-PAGE analysis of different PSII preparations and LHCII. Samples containing 2, 1 and 0.5 μg chlorophylls were loaded for each sample (lane 1, 1/2 and 1/4 under "BBY", "MCC" and "CC"). (B) Western blot analysis with antibodies against individual antenna proteins Lhcb1-6 to analyze the outer antenna composition in different PSII preparations. CP47 was chosen as a reference. For the immunoblotting of Lhcb1-5 and CP47, samples containing 0.5, 0.25 and 0.125 μg chlorophylls were loaded (lane 1, 1/2, 1/4 under "BBY", "MCC" and "CC"). For the immunoblotting of Lhcb6, four times more samples (each containing 2, 1 and 0.5 μg chlorophylls) were loaded for each sample. (C) Absorption spectra of different PSII preparations and LHCII complex measured at room temperature. The spectra are normalized to the maxima in the Q_y region. (D) 77 K fluorescence emission spectra of different PSII preparations and LHCII. Excitation was at 436 nm, and spectra were normalized to their maxima.

ratio as the corresponding co-reconstituted samples and were used as negative controls for assessing possible energy transfer caused by simple close physical distance between different vesicles, rather than by intra-vesicular protein–protein interaction in the membrane.

Three different experiments were performed to verify proper incorporation of the different proteins into liposomes and the interaction between LHCII and the PSII core complexes in co-reconstituted proteoliposomes, namely: 1) Nycodenz density gradient centrifugation followed by TLC and SDS-PAGE analysis for lipids and protein compositions; 2) freeze-fracture electron microscopic analysis to the structure of the proteoliposomes; and 3) MS-based chemical cross-linking for protein interaction analysis.

Nycodenz density gradients of all reconstituted samples resulted in three bands, reflecting the distribution of proteoliposomes with different protein densities or different proteoliposome diameters (Fig. 2A). Empty liposomes floated on the top of the gradients were best visible against a black background (Fig. S3). The lipid compositions of the three bands were determined by TLC (Fig. 2B and C). Each band contained four types of lipids whose ratio was approximately the same as that in the reference lipid mixtures (MGDG/DGDG/PG/SQDG = 50/30/12/8 (w/w/w/w)), which indicated conservation of lipid composition ratio during proteoliposome reconstitution procedure. The protein composition of the proteoliposomes was checked by Tricine-SDS-PAGE (Fig. 2D and E). Proteoliposomes containing only MCC showed the expected bands of the PSII core complex including the minor antennae, and those of co-reconstituted proteoliposomes with LHCII showed, in addition, the respective bands indicating the successful co-incorporation of LHCII and MCC into the membrane (Fig. 2D). CC proteoliposomes lacked the minor antenna proteins but also showed clearly that the LHCII and CC were co-incorporated successfully into proteoliposomes (Fig. 2E). The freeze-fracture microscopic analysis (Fig. 2F) supports that the proteins have been inserted properly into the membrane bilayer and that the particles are dispersed evenly.

Table 1
The oxygen evolution rates (μmol O_2/mg Chl/h) of PSII preparations and the corresponding proteoliposomes measured under different light intensities[a].

	1200 μmol photons/m^2/s	3900 μmol photons/m^2/s
BBY	324.7 ± 4.1	537.8 ± 17.3
MCC	329.5 ± 12.9	527.2 ± 24.5
MCC PL	351.3 ± 7.0	619.6 ± 28.8
CC	613.4 ± 13.4	1387.1 ± 38.3
CC PL	700.2 ± 5.4	1719.4 ± 43.1

[a] All data are the average of 3 independent measurements.

The interaction between LHCII and the PSII core complexes in the membrane were analyzed by chemical cross-linking analysis followed by LC–MS/MS. SDS-PAGE (Fig. 3) recognized two apparently cross-linked products, with molecular masses of 50 kDa and 70 kDa, in both the MCC–LHCII and CC–LHCII proteoliposomes. The 50 kDa products might represent the dimer of intermolecular linked LHCII subunits. The 70 kDa products might be the intermolecular link of LHCII and PSII core subunits. There were also a few faint bands between 50 kDa and 100 kDa and several bands with larger molecular masses above 100 kDa. However, similar chemical cross-linked products were also recognized in the lane of samples containing a mixture of LHCII PL and

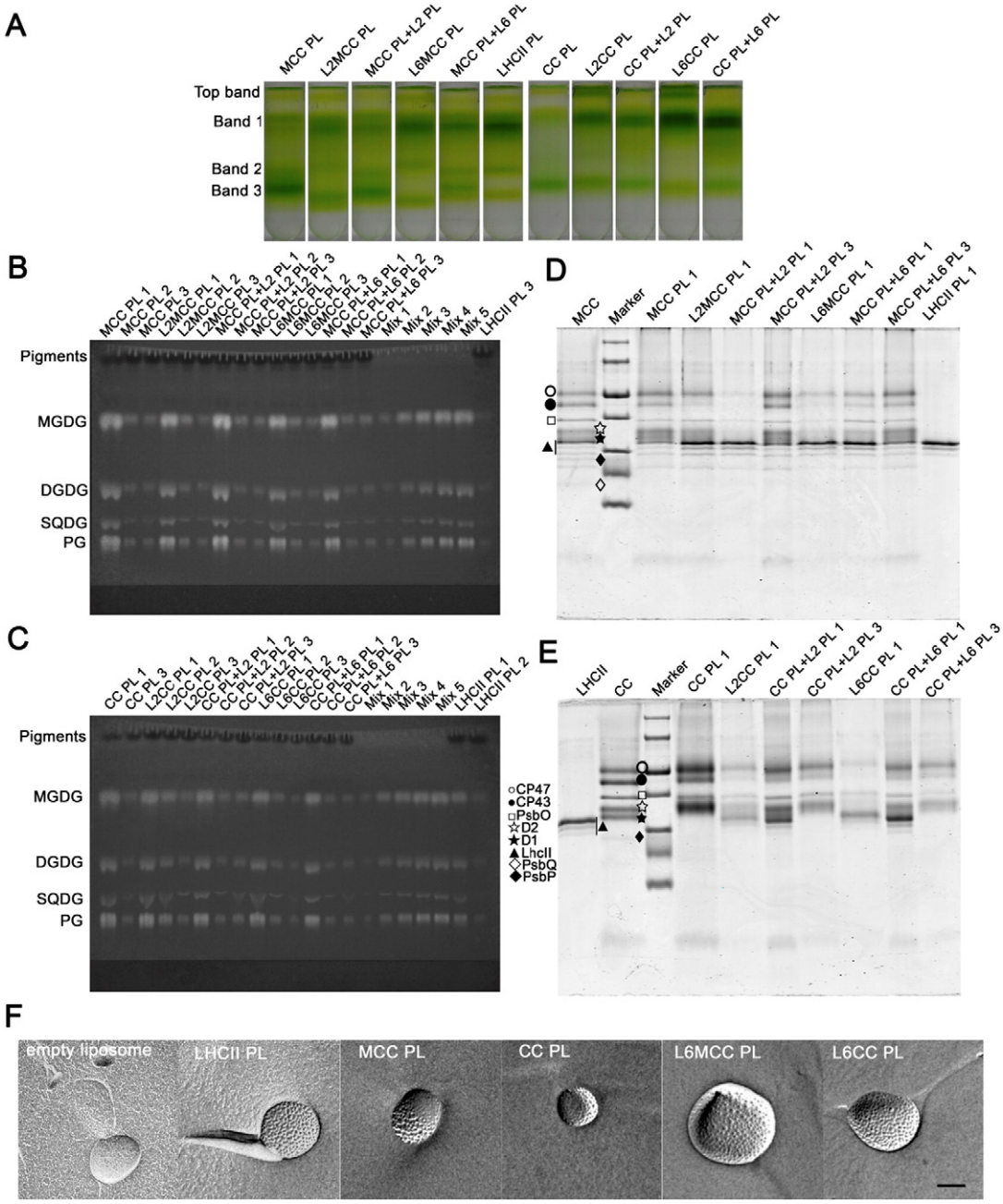

Fig. 2. Incorporation of LHCII and the PSII core complexes into liposomes. (A) Flotation of different proteoliposomes in the Nycodenz density gradient. Samples in 7.5% Nycodenz were loaded on a 10–40% Nycodenz density linear gradient. (B–C) TLC analysis to lipid composition of the Nycodenz density gradient bands corresponding to the proteoliposomes. Lipid samples with the same chlorophyll amount were loaded onto the silica gel plates. Lipid mixtures (Mix 1–Mix 5) containing 2, 8, 14, 20 and 26 μg lipids were loaded as reference. (D–E) Tricine-SDS-PAGE analysis of green bands harvested from (A). Sample containing 0.75 μg chlorophylls was loaded on each lane. (F) Freeze-fractured electron microscopy of empty liposomes and different proteoliposomes. Scale bar: 100 nm.

CC PL proteoliposomes. The cross-linking products were immunoblotted with antibody against Lhcb1, which further identified that both the 50 kDa and 70 kDa cross-linking products contained LHCII subunits (Fig. S4A). Because of the unspecific interaction of the Lhcb1 antibody, LC–MS/MS was performed to further identify the intermolecular cross-linking; especially the cross-linked products including both LHCII and PSII core subunits (Fig. 4). Since the cross-linker used in this study, Sulfo-EGS, reacts with the primary amino groups and is water-soluble, exposed residues were candidates for the reaction. Although there are 12 lysine residues in the Lhcb1 apoprotein, only the three lysine residues (K2, K7 and K8) near the N terminus can possibly serve as the potential sites for chemical cross-linking. The others are located either in the transmembrane region or in hydrophobic region close to membranes, where the cross-linking is unlikely to occur. There are several lysine residues on both the stromal and luminal sides of CP47. In addition, the luminal extrinsic PSII subunits, PsbO, PsbP and PsbQ, contain abundant lysine residues. The subunits on the lumen side of PSII protrude considerably in the hydrophilic environment, and thus can easily be cross-linked by a water-soluble cross-linker. The results of LC–MS/MS demonstrated that the K8 residue near the N terminus in Lhcb1 was cross-linked with K504 of CP47, both are located on the stromal side of thylakoid membrane (Fig. 4). Chemical cross-linking between LHCII and CP47 verified the co-reconstitution of LHCII and the PSII core complexes. K8 of LHCII was also found cross-linked with lysine residues on the luminal side of CP47 (K419) and K5 of PsbO (Fig. S5), which indicated that some PSII core complexes and LHCII were incorporated in an anti-parallel orientation

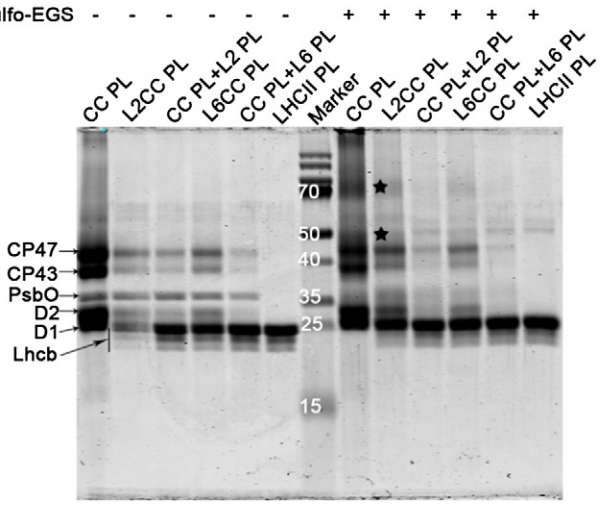

Fig. 3. Tricine-SDS-PAGE analysis of the Sulfo-EGS cross-linking between LHCII and the PSII core complexes in the CC–LHCII proteoliposomes. Sample containing 2 μg chlorophylls was loaded on each lane.

in the proteoliposomes. Cross-linking between LHCII and PSII core complexes, together with the freeze-fracture electron micrographs, confirmed the co-incorporation of LHCII and the PSII core complexes into the liposome membranes.

3.3. Incorporation of MCC and CC into liposomes enhanced their photochemical activities

The influence of incorporating the PSII core complexes into liposomes on their structural and functional characteristics was investigated by fluorescence emission spectroscopy and oxygen evolution capacity. The incorporation of MCC or CC individually into lipid membranes did not change their main fluorescence emission peaks (Fig. S6). Rather, incorporating CC into liposomes markedly reduced the long wavelength (>700 nm) fluorescence emission. Judged by the oxygen evolution rate (Table 1), the photochemical activities of the PSII core preparations were significantly enhanced when incorporated into the lipid bilayer. When measured at 1200 μmol photons/m^2/s, the oxygen evolution activities of MCC and CC increased by 7% (from 329.5 ± 12.9 to 351.3 ± 7.0 μmol O_2/mg Chl/h) and 14% (from 613.4 ± 13.4 to 700.2 ± 5.4 μmol O_2/mg Chl/h), respectively. When measured at higher light intensity (3900 μmol photons/m^2/s), the oxygen evolution activities of MCC and CC increased by 18% and 24%, respectively.

3.4. Energy transfer from LHCII to the PSII core complex in proteoliposomes

77 K fluorescence emission spectra of different proteoliposomes, sensitized by Chl *a* (436 nm), do not present significant changes between the co-reconstituted proteoliposomes compared with their negative control counterpart consisting of the mixture of LHCII PL and CC PL (Fig. 5A and C). The proteoliposomes containing more LHCII present a slight blue-shift in the 77 K fluorescence emission, compared with those containing relatively less LHCII (Fig. 5A and C). However, the samples differed when they were excited by 480 nm light which is absorbed preferentially by Chl *b* (Fig. 5B and D). The fluorescence spectra of the mixtures of CC proteoliposomes and LHCII proteoliposomes peaked at shorter wavelengths (683.4 nm for CC PL + L2 PL and 682 nm for CC PL + L6 PL) and contained higher 700 nm emission intensities than the co-reconstituted proteoliposomes (684.4 nm and 683 nm in L2CC PL and L6CC PL, respectively). Fig. 5 shows that the proteoliposomes containing LHCII exhibited increased fluorescence emission in the 710–750 nm range. This may be attributed to low energy states resulting from conformational disorder of LHCII [54]. Meanwhile, their intensities at 700 nm were higher. These features clearly represent the characteristics of the fluorescence of uncoupled LHCII in LHCII PL (Fig. 5).

Gaussian deconvolution of 77 K fluorescence emission spectra of different proteoliposomes gave five components: F680, F685, F695, F700, and F730, which were assigned to the fluorescence emissions of LHCII, PSII RC-CP43, CP47, LHCII aggregates, and from overlapping low-energy vibrational side bands, respectively [54,55]. There are no remarkable differences in F695 and F730 among the different proteoliposomes. The changes in the components F680, F685, and F700 mainly reflect the excitation energy distribution between LHCII and PSII RC. Fig. 6C and D shows the Gaussian components of the emissions of all proteoliposomes excited at 436 nm (Chl *a*) and 480 nm (Chl *b*). Several characteristics are remarkable: 1) compared with the proteoliposomes mixtures, the corresponding co-reconstituted PSII–LHCII proteoliposomes had a larger F685 component (PSII RC) and a correspondingly decreased component arising from uncoupled LHCII (F680 and F700),

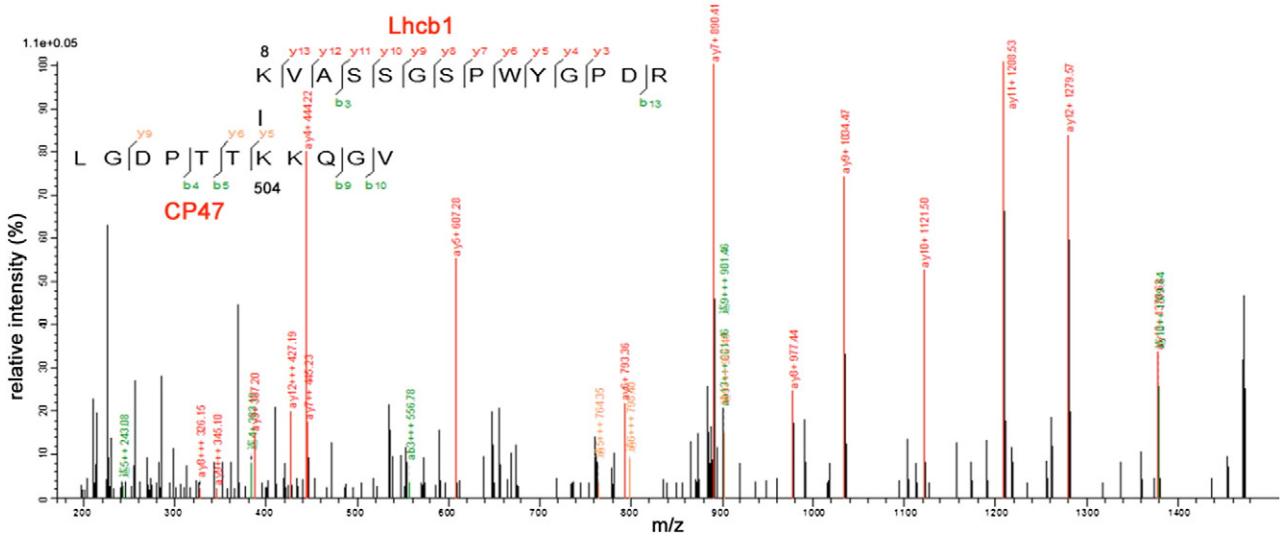

Fig. 4. The LC–MS/MS of cross-linked peptides. Product ion map of cross-linked peptides K^{8}VASSGSPWYGPDR (Lhcb1) and LGDPTTK^{504}KQGV (CP47). The precursor ions showing cross-linking were m/z = 955.1454 (3+).

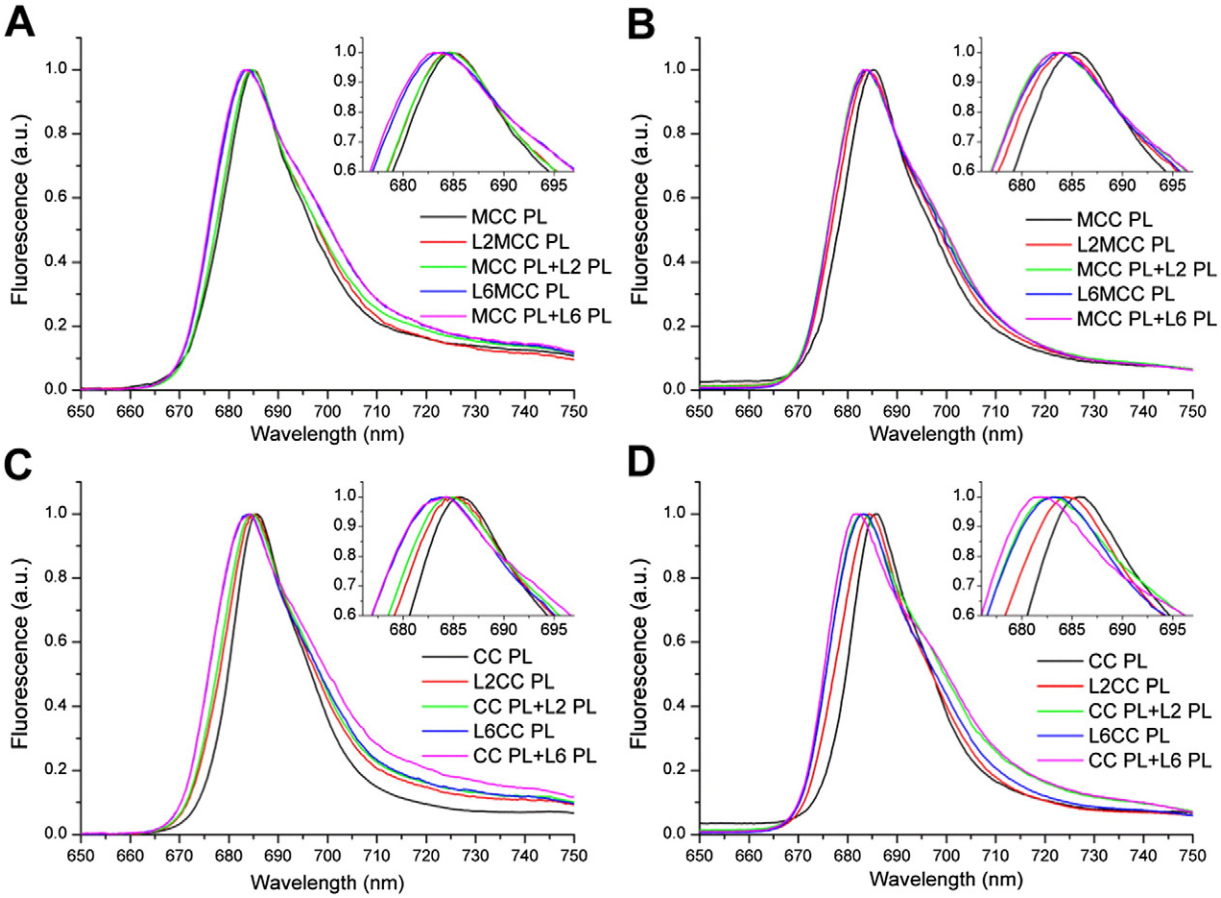

Fig. 5. 77 K fluorescence emission spectra of different PSII proteoliposomes. (A–B) Fluorescence emission spectra of MCC-containing proteoliposomes measured upon Chl *a* excitation (A) and upon Chl *b* excitation (B). (C–D) Fluorescence emission spectra of CC-containing proteoliposomes measured upon Chl *a* excitation (C) and upon Chl *b* excitation (D). Spectra were normalized to their maxima.

indicating energy transfer from LHCII to the PSII core complex in the co-reconstituted PSII–LHCII proteoliposomes; 2) the excitation distribution in CC-LHCII proteoliposomes varied significantly under different excitations. With excitation at 480 nm, more energy was distributed to PSII RC than with excitation at 436 nm; 3) increasing the incorporation of LHCII in the proteoliposomes, the areas under the bands of F680 and F700 components increased significantly and correspondingly, the F685 component decreased, indicating an increase of uncoupled LHCII in these proteoliposomes.

Furthermore, Chl *a* fluorescence induction kinetics in the presence of DCMU were measured according to Malkin et al. [56], and modified for evaluating the energetic coupling between light-harvesting system and PSII RC in the co-reconstituted proteoliposomes. When electron transfer from Q_A to Q_B is blocked by DCMU, the rate of fluorescence rise is positively correlated with the Q_A reduction rate, which is related directly to the charge separation rate in PSII RC, depending on the effective antenna size of PSII and the energy transfer efficiency from the antenna system to PSII RC [57,58]. Fig. 7A and B shows the Chl *a* fluorescence induction kinetics of different proteoliposomes treated with DCMU. The simple proteoliposome mixtures presented similar fluorescence induction kinetics as the corresponding PSII proteoliposomes (CC PL + L2 PL and CC PL + L6 PL vs CC PL; or MCC PL + L2 PL and MCC PL + L6 PL vs MCC PL, respectively). On the contrary, the fluorescence induction of co-reconstituted PSII–LHCII proteoliposomes was much faster than that of the respective PSII core proteoliposomes, which demonstrated that excitation was transferred from LHCII to PSII RC in the co-reconstituted proteoliposomes. Among all proteoliposomes, L6MCC PL showed the fastest fluorescence induction and the L6CC PL the second fastest. The antenna cross-section of PSII in different proteoliposomes was estimated based on the average time ($\tau_{2/3}$) corresponding to 2/3 of the fluorescence induction maxima (Fig. 7C and D). The antenna cross-section of MCC PL was more than twice as large as that of CC PL, suggesting that there were more antennae in MCC, which was in agreement with the result of the protein composition analysis (Fig. 1). All MCC–LHCII proteoliposomes presented larger antenna cross-section compared with the corresponding CC–LHCII ones, e.g. the antenna cross-section of the L2MCC PL was about 1.5 times larger than that of the L2CC PL, and L6MCC PL 1.2 times larger than that of L6CC PL. Increasing the amount of LHCII from 0 to 6 trimers per PSII RC for co-reconstitution increased the amount of effective LHCII coupling to PSII, especially for the proteoliposomes without minor antennae. The antenna cross-section increased by 51% and 85% for L2MCC PL and L6MCC PL, respectively, compared with those of the MCC PL. For CC–LHCII proteoliposomes, the functional antenna size of L2CC PL was almost doubled and that of L6CC PL even quadrupled compared with that of the CC PL. In conclusion, the Chl *a* fluorescence induction kinetics measurement revealed two phenomena: 1) all proteoliposomes with minor antennae presented larger antenna-cross-section compared with the individual counterpart without minor antenna, implying a role of the minor antennae in the stabilize the structure of PSII supercomplexes; 2) the lack of minor antenna between did not block energy transfer from the major antenna to the PSII core complex, nor did it inhibit the coupling of increased amount of major antenna to PSII.

In order to investigate the effect of the minor antennae on photochemical activities of the PSII complexes, DCPIP photoreduction rates of different proteoliposomes were measured in the presence of the electron donor DPC, under either white or blue light irradiation

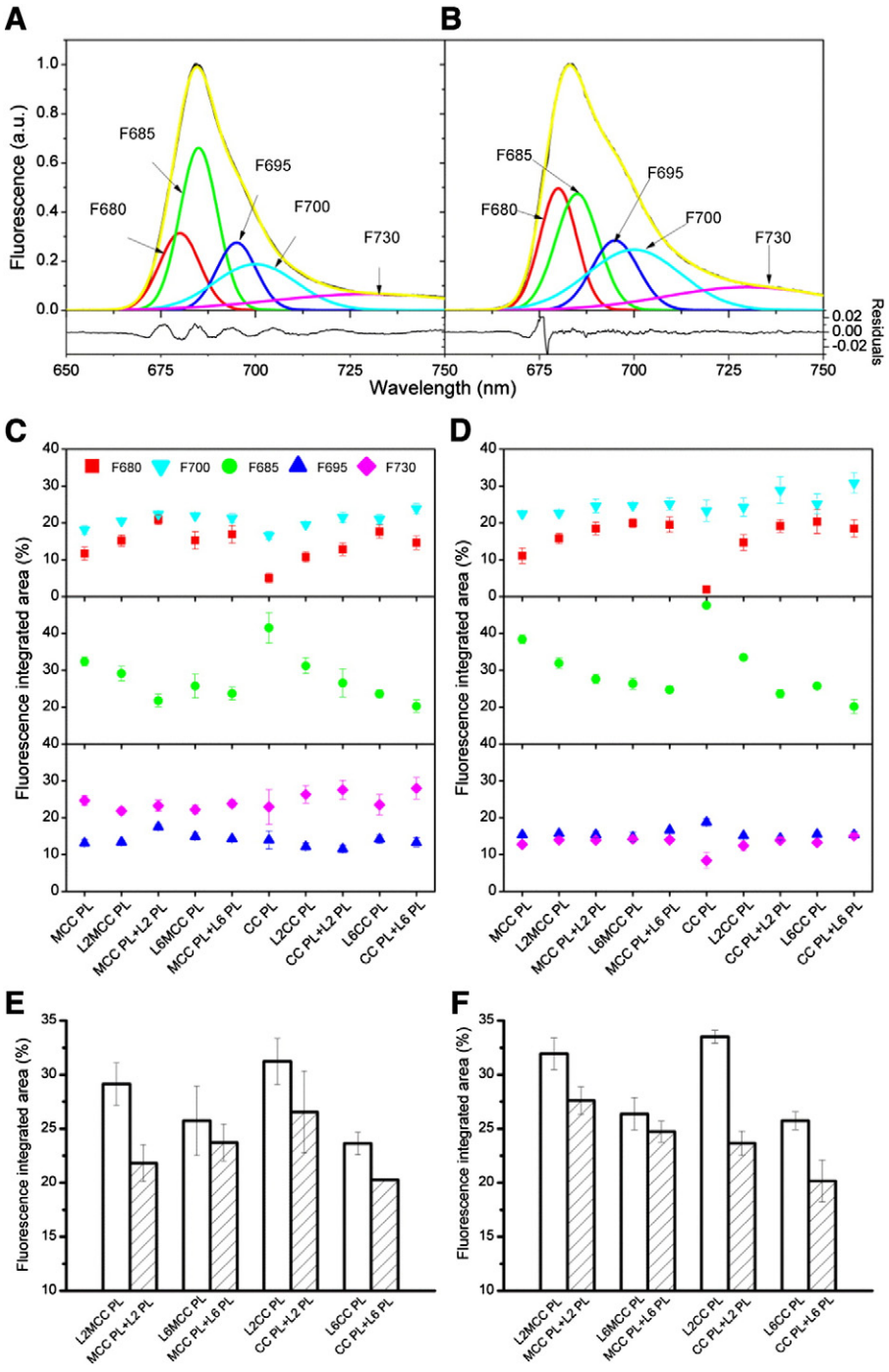

Fig. 6. Gaussian deconvolution of 77 K fluorescence emission spectra of different PSII proteoliposomes. Spectra were decomposed into 5 components: F680, F685, F695, F700 and F730, representing the weight of subspectra peaking at 680 nm, 685 nm, 695 nm, 700 nm and 730 nm, respectively. (A–B) Examples of the deconvolution of spectra measured upon Chl *b* excitation (480 nm). (A) Co-reconstituted proteoliposome L2CC PL, and (B) proteoliposome mixture CC PL + L2 PL. (C–D) Relative contribution of the individual Gaussian components to the emission spectra excited at 436 nm (C) and 480 nm (D). (E–F) Comparison of the relative contribution of the F685 components of co-reconstituted proteoliposomes with the respective proteoliposome mixtures excited at 436 nm (E) and 480 nm (F). Data are derived from 3 individual measurements.

(Fig. 8). The photoreduction of DCPIP is a process that involves energy transfer, charge separation and electron transport. The results should be considered as the consequence of combined effects from several determinants. Any uncoupled LHCII in the system may negatively influence the DCPIP photoreduction rate by virtually reducing the incident light intensity that resulted from the competitive absorption of light (Fig. S7). To compensate for this effect, the simple mixtures of LHCII proteoliposomes and PSII core proteoliposomes containing the same amount of pigment–protein complexes as the respective co-reconstituted ones were used again as negative controls.

Fig. 8A shows the comparison of DCPIP reduction rates of different proteoliposomes under white light, exciting both peripheral antenna and the PSII core complexes. Compared with its negative control (MCC PL + L2 PL), the DCPIP reduction activity of L2MCC PL was slightly higher, which may indicate the contribution of the increased antenna cross-section to the photochemical activity of the PSII core. However, DCPIP reduction activity of L6MCC PL was significantly lower than that of MCC PL + L6 PL (Fig. 8A), indicating that the further increased antenna cross-section may function as an energy quencher in this case. In contrast, when the minor antennae were absent, there was no

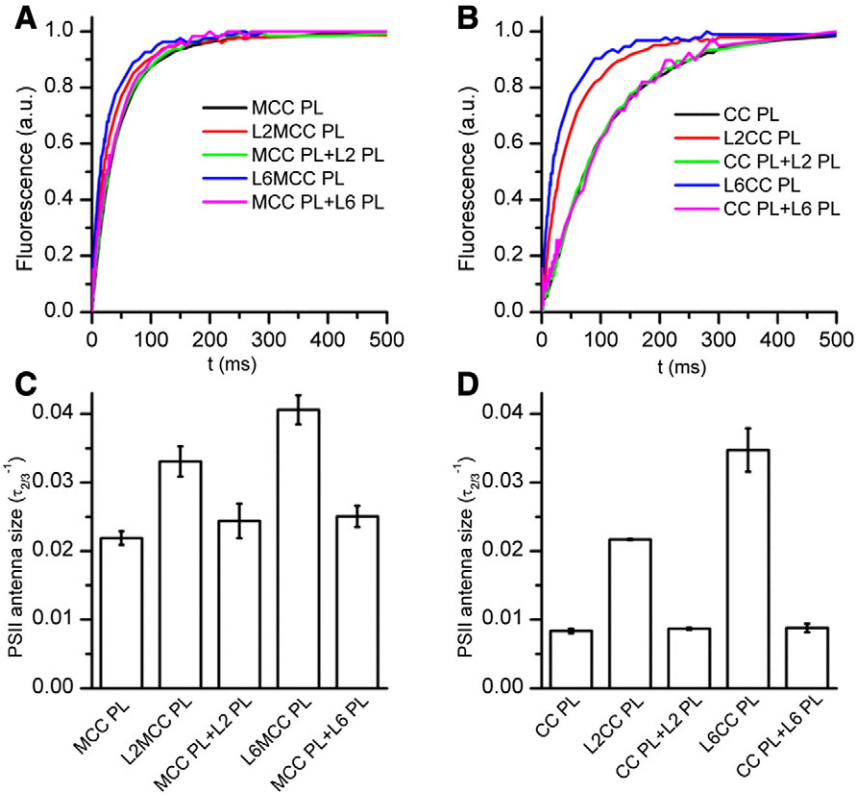

Fig. 7. Chlorophyll *a* fluorescence induction kinetic analysis of different PSII proteoliposomes. (A–B) Chl *a* fluorescence induction kinetics of MCC-containing proteoliposomes (A) and CC-containing proteoliposomes (B). Chl *a* fluorescence was induced by broad green excitation light switched on at 0 s and was normalized to the steady state level. (C–D) Apparent PSII antenna sizes in MCC-containing proteoliposomes (C) and CC-containing proteoliposomes (D). Data presented are inversely proportional to the time required for reaching 2/3 of the maximum fluorescence. Data are derived from 3 individual measurements.

difference between the DCPIP photoreduction rates of the L2CC PL and CC PL + L2 PL, or L6CC PL and CC PL + L6 PL under the white light. Apparently, in the absence of minor antennae, energy absorbed by the peripheral antenna did not affect photochemical activity of PSII RC in the CC–LHCII proteoliposomes under white light excitations.

MCC–LHCII proteoliposomes showed a similar behavior as those under the white light condition when the DCPIP photoreduction rates of the same samples were measured under blue light (465–485 nm LED with 480 ± 2 nm narrow bandpass filter) that predominantly excites Chl *b* and carotenoids (Fig. 8B). In contrast, CC–LHCII proteoliposomes showed a remarkable effect of the enhanced antenna cross-section on DCPIP reduction rates compared with their corresponding negative controls (CC PL + L2 PL and CC PL + L6 PL) (Fig. 8B). Apparently, the effect of enhanced antenna cross-section on the photochemical activities was only visible if the antenna was predominantly excited.

Observing the overall DCPIP reduction rates of different proteoliposomes revealed two different common phenomena: 1) the overall DCPIP reduction activities of CC–LHCII proteoliposomes were lower than those of the MCC–LHCII proteoliposomes, which implied a contribution of the minor antennae in the photochemical activity of PSII; 2) although all the proteoliposomes containing 6 LHCII per PSII dimer showed larger antenna cross-sections than the ones containing only two LHCII per PSII dimer, they did not necessarily result in higher DCPIP reduction rates. This leads to the hypothesis that the increased LHCII in the proteoliposomes has an energy quenching effect. The competition effect of increased LHCII in the system for incident light was confirmed by a titration experiment: the photoreduction activities of MCC PL markedly decreased when the amount of LHCII in the system increased (Fig. S7), which might also be partly responsible for the decrease of DCPIP reduction activity with the increased amounts of co-inserted LHCII.

4. Discussion

4.1. The photochemical activity of PSII is enhanced in the liposome membrane environments

Oxygen evolution activity measurement demonstrated that all PSII preparations (BBY, MCC and CC) retain the capacity for oxygen evolution, irrespective of the differences in antenna composition and cross-section. The results of oxygen evolution rate of BBY and CC were in agreement with previous studies [40,42]. The MCC studied in this work showed much lower oxygen evolution activities than the OctGlc cores obtained by Hankamer et al. [42]. This may be due to the fact that MCC had a much lower Chl *a*/*b* value compared to the OctGlc cores (4.2 vs 10.2), that is, the amount of its RC was much lower than that of the OctGlc cores based on the same Chl amount. Accordingly, two different PSII preparations, MCC with minor antennae and CC without any antenna were both functionally intact. Together with the purified LHCII, they provided the basis of the proteoliposome reconstitution for studying the interaction between the PSII core complex and the peripheral antenna system, especially the function of the minor antenna.

The incorporation of MCC or CC into the liposome membrane promotes the photochemical activities of the PSII complexes (Table 1). The oxygen evolution activities of the MCC and CC, upon insertion into the membrane environments, increased about 7% and 14%, respectively, when measured at 1200 μmol photons/m^2/s light. The oxygen evolution activities increased more significantly when measured at saturated light. The oxygen evolution rates of MCC and CC increased by 18% and 24%, respectively. Together with the result of low temperature fluorescence emission spectra (Fig. S6), this indicates that the membrane not only retains, but also improves PSII functions. This may be due to the lateral pressure in the membrane exerted by the non-bilayer-forming lipid MGDG [59–61].

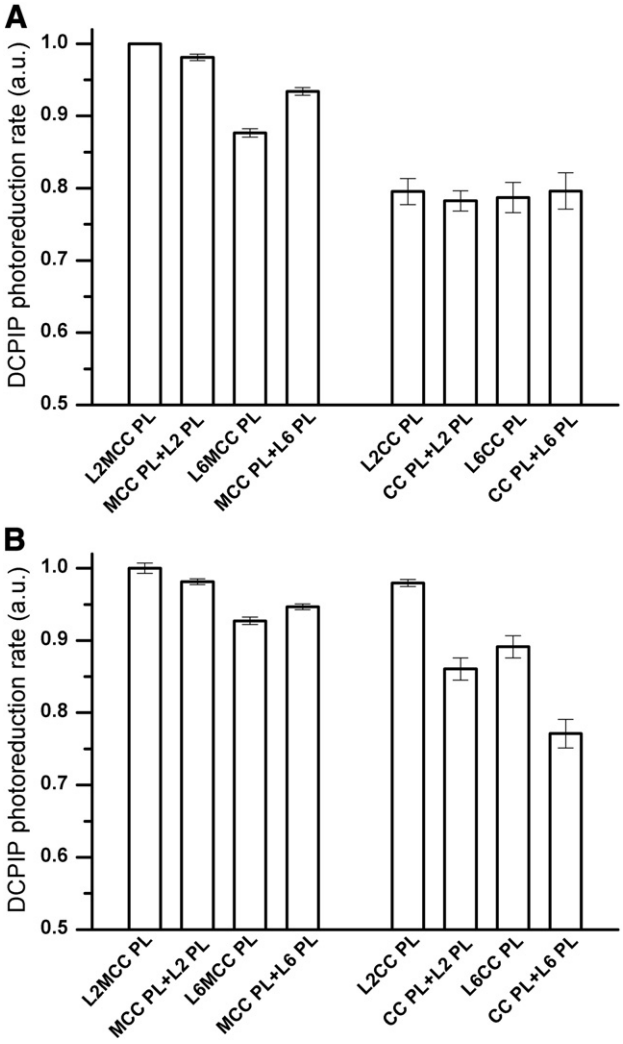

Fig. 8. The comparison of photochemical activities of different PSII proteoliposomes measured by DCPIP photoreduction rate under white light (A) or blue light (B). The data were normalized to the maximum. The data and standard deviation are derived from 3 individual measurements.

4.2. The PSII core complex and LHCII undergo protein–protein interaction upon their co-incorporation into liposomes

The cross-linking between the subunits of CC and LHCII detected by LC–MS/MS provided evidence for the interaction of LHCII and the PSII core complexes in the absence of the minor antennae (Fig. 4). Unlike the vertical interaction between phycobilisomes (PBS) and the PSII core complex in cyanobacteria [62], th ecross-linking of CC with LHCII in the proteoliposomes deals with the interaction between two proteins embedded side-by-side in the membrane. The distance between LHCII and the PSII core complexes of higher plants are larger [63] and the interaction between them may be weaker than those between PBS and the PSII core in cyanobacteria. Because of this, the 16.1 Å cross-linker Sulfo-EGS was chosen to investigate the interaction between LHCII and the PSII core complexes in liposome membranes. CC–LHCII proteoliposomes were chosen for chemical cross-linking reaction because it is impossible for MCC–LHCII proteoliposomes to distinguish the incorporated LHCII and residual LHCII retained in MCC (Fig. 1).

While the PSII core complex and LHCII are uniquely oriented in thylakoids, parallel (= natural) and anti-parallel orientations are likely to be present in the reconstituted membranes. This is supported by peptides resulting from the cross-linking of the stromal lysine residue of Lhcb1 which was found to be cross-linked with the luminal lysine residues of CP47 or PsbO (Fig. S5). It is known that LHCII incorporated into lipid bilayers in a random (up or down) orientation [64], hence, it can be assumed that LHCII and the PSII core complexes could take either a parallel orientation or an anti-parallel orientation in the co-reconstituted proteoliposomes. Due to the dense pigment packing, it is likely that energy transfer is not only possible in the parallel arrangement. Therefore any increase in antenna size measured in this work would then represent a lower limit; a true quantification would require incorporation of all proteins in a parallel orientation. It is, however, likely that it is less efficient in the anti-parallel arrangement because of the unique energy transfer pathways in PSII [19,63,65]. It was proposed that energy absorbed by lumenal Chl clusters maybe transferred to the stromal Chl clusters, from which energy flow to the terminal site [44]. Nield and Barber [65] proposed that the energy transfer pathway from LHCII to the PSII core are directly related to the terminal site (the Chl cluster Chl610–611–612) in LHCII [66,67]. Caffarri et al. also proposed two possible energy transfer pathways from the peripheral antenna to the PSII core complex: S-LHCII trimer and CP26 could transfer energy to Chls in CP43 through Chls 611/612. Alternatively, CP24 and M-LHCII trimer could transfer energy to Chl 511 in CP47 through CP29 [63]. This further illustrates that the positions and orientations of LHCII relative to the PSII core complex are important for energy transfer from LHCII to the PSII core complex. Therefore, it can be assumed that the energy transfer observed in the PSII–LHCII proteoliposomes was from the complexes that were incorporated in parallel orientations in the membrane.

4.3. The major antenna can transfer energy to the PSII core complexes in the absence of minor antenna in liposomes

Studies on the mutants lacking one or two minor antennae provided evidences that lack of CP29 or CP24 reduced maximal photosynthetic efficiency of PSII, or increased the energy migration time from LHCII to the PSII core [23,26–28,30]. Recently, an *A. thaliana* mutant line lacking all minor antennae was obtained, whose functional connection between LHCII and PSII core complexes in the thylakoid membrane was impaired [32]. Although the efficiency of energy transfer from the major antenna to the RC was less and the energy migration time was delayed, all of these results indicated that the absence of the minor antenna did not block the energy transfer from the peripheral antenna to the reaction center completely.

In this study, we demonstrated that in a reconstitution system the lack of the minor antenna between LHCII and PSII core complexes did not block the energy transfer from LHCII to the PSII core complexes. The estimation of the antenna cross-section to CC PL, L2CC PL, or L6CC PL (Fig. 7) indicated clearly that the incorporation of LHCII to CC enhanced the antenna cross-section of PSII significantly. These results was further supported by the deconvolution of the 77 K fluorescence emission spectra, which showed the markedly enhanced excitation distribution to the PSII core in the L2CC PL or L6CC PL compared with that of the corresponding simple mixture of LHCII PL and CC PL (Fig. 6), which clearly indicated that the energy absorbed by LHCII was transferred to PSII RC in the co-reconstituted proteoliposomes. Although there was a very small amount of CP26 detected in CC (0.0083 CP26 per PSII core complex), this is not expected to have a large effect on the interaction between LHCII and the PSII core complex. If we assume that only those LHCII are bound to PSII core complex via a minor antenna such as CP26 can transfer excitation energy to PSII RC, and that each CP26 in the CC preparation functions as a bridge coupling one LHCII trimer to the PSII core complex, then still less than 1% of the core complexes receive excitation energy from LHCII. Taking into account that the PSII core complex contains more Chls than one LHCII trimer, then the absorption cross-section of the PSII core complex should increase by less than 1% upon the addition of LHCII. However, the functional antenna size of L2CC PL was almost doubled and that of L6CC PL even quadrupled compared with that of CC PL (Fig. 7D). This

result indicates strongly that it is impossible that only the remained Lhcb5 functions as a bridge between LHCII and PSII RC in the CC-containing proteoliposomes. Therefore, LHCII trimers must be able to couple directly to the PSII core complexes.

This study also demonstrated that the PSII core complex can couple energetically with LHCII trimers in the absence of the minor antennae in liposomes. Increasing the LHCII/PSII ratio from two (L2CC PL) to six (L6CC PL) in proteoliposomes resulted in enormously enhanced antenna cross-section of the PSII core (Fig. 7). Compared with the MCC–LHCII proteoliposomes, the CC–LHCII proteoliposomes showed a more pronounced F685 component in the 77 K fluorescence emission spectra and stronger increase in the antenna cross-section upon incorporation with an increased amount of the major antennae (Figs. 6 and 7). Actually, the PSII–LHCII supercomplexes are capable of carrying out structural adjustment when one or more minor antennae are missing. Cross-linking between K8 of Lhcb1 and K504 of CP47 provided evidence for the assembly of PSII supercomplexes in the absence of minor antennae (Fig. 4) and it also implied that the location of LHCII may be the position of M-LHCII. However, we could not exclude other possible locations of LHCII in the CC–LHCII proteoliposomes because of the small number of detectable of chemical cross-linking events. De Bianchi et al. [23] have observed that in the absence of CP29, the S-LHCII binding to the PSII core bent toward the CP47 and interposed into the space of CP29. This kind of modification in the S-LHCII binding mode may change the pathway for LHCII to transfer excitation energy directly to PSII RC via CP43 [23,65]. The hypothetical basic PSII supercomplex model $C_2S_2M_2$ suggested by Boekema et al. [18] proposes that the minor antennae in the interface of LHCII and the PSII core stabilize the overall architecture of PSII–LHCII supercomplexes, which improves the harvesting of solar energy and allows adjusting it to the ever-changing environmental light conditions. Drop et al. also proposed that some of the antennae (CP24 or Lhcb3) may have evolved not for increasing the antenna cross-section, but rather for a more effective controlling of the PSII super-molecular regulation under different environmental conditions [29]. The minor antennae in the proposed model may be more important in the sense of a modulator regulating the energy exchange between LHCII and PSII core complexes, rather than being an indispensable energetic coupling element between them.

4.4. Minor antennae play important roles in photochemical activities of PSII

An increased antenna cross-section of PSII RC in the co-reconstituted liposomes has been clearly demonstrated, through both increased the excitation distribution to PSII RC and increased Chl *a* fluorescence induction rate in the proteoliposomes (Figs. 6 and 7), that energy can be transferred from LHCII to the PSII core complexes. The effects, however, did not show a straightforward correlation with the photochemical activities of PSII RC (Fig. 8). For the CC–LHCII proteoliposomes, the effects of enhanced antenna cross-section on photochemical activity were completely different under white and blue light. This might be attributed to the enhanced difference in the gap of free energy between LHCII and PSII RC [68] under blue light, when the excitation in the PSII core is small since only the carotenoid still absorbs energy. The fact that MCC–LHCII supercomplexes did not show the same phenomenon, under blue light, suggests that the energy absorbed by the minor antennae between LHCII and PSII already satisfied the capacity of PSII under these conditions [69]. The DCPIP reduction is a process influenced by a variety of factors including the charge separation rate, the rate of the energy migration from peripheral antenna to PSII RC, and the activity of oxygen evolution reaction [70], which implies that, the increased antenna cross-section might not necessarily result in the increase of photochemical activity of PSII. In this study, the effect of the increased antenna cross-section on the photoreduction reaction of PSII can be observed; only if the excitation energy in PSII RC is too low such that the energy transfer from the peripheral antenna to PSII RC becomes a limiting factor. In this sense, the DCPIP reduction experiment of CC–LHCII proteoliposomes under blue light condition provided another evidence for an effective energy transfer from LHCII to the PSII core.

In addition, it is noteworthy that the DCPIP reduction activities of MCC-containing proteoliposomes were higher than those of CC-containing proteoliposomes (Fig. 8). It denotes the functionality of the minor antennae in keeping the integrity of the PSII photochemical unit, which is in agreement with former observations [27,28,32].

Acknowledgements

This work was supported by the National Basic Research Program of China (No. 2011CBA00904 to CY), the Knowledge Innovation Program of the Chinese Academy of Sciences (KSZD-EW-Z-018 to CY), the National Natural Science Foundation of China (Nos. 31070212 and 31370275 to CY), and the Deutsche Forschungsgemeinschaft (SFB 625-TP B7 to HP). We thank Prof. Hugo Scheer (Ludwig-Maximillian University) for his creative discussion and his critic reading of the manuscript, Dr. Helmut Kirchhoff (Washington State University) for advice in Chl *a* fluorescence induction kinetics measurement, Dr. Shufeng Sun (Institute of Biophysics, CAS) and Prof. Yilin Sun (Beijing Neurosurgical institute) for the help in freeze-fracture electron microscopy, and Dr. Zhuang Lu (Institute of Botany, CAS) for support in LC–MS/MS.

Appendix A. Supplementary data

Supplementary data to this article can be found online at http://dx.doi.org/10.1016/j.bbabio.2014.11.005.

References

[1] J. Barber, Photosystem II: the engine of life, Q. Rev. Biophys. 36 (2003) 71–89, http://dx.doi.org/10.1017/S0033583502003839.
[2] C. Pagliano, G. Saracco, J. Barber, Structural, functional and auxiliary proteins of photosystem II, Photosynth. Res. 116 (2013) 167–188, http://dx.doi.org/10.1007/s11120-013-9803-8.
[3] Y. Umena, K. Kawakami, J.R. Shen, N. Kamiya, Crystal structure of oxygen-evolving photosystem II at a resolution of 1.9 Å, Nature 473 (2011) 55–60, http://dx.doi.org/10.1038/nature09913.
[4] A. Guskov, J. Kern, A. Gabdulkhakov, M. Broser, A. Zouni, W. Saenger, Cyanobacterial photosystem II at 2.9 Å resolution and the role of quinones, lipids, channels and chloride, Nat. Struct. Mol. Biol. 16 (2009) 334–342, http://dx.doi.org/10.1038/nsmb.1559.
[5] B. Loll, J. Kern, W. Saenger, A. Zouni, J. Biesiadka, Towards complete cofactor arrangement in the 3.0 Å resolution structure of photosystem II, Nature 438 (2005) 1040–1044, http://dx.doi.org/10.1038/nature04224.
[6] K.N. Ferreira, T.M. Iverson, K. Maghlaoui, J. Barber, S. Iwata, Architecture of the photosynthetic oxygen-evolving center, Science 303 (2004) 1831–1838, http://dx.doi.org/10.1126/science.1093087.
[7] N. Kamiya, J.R. Shen, Crystal structure of oxygen-evolving photosystem II from *Thermosynechococcus vulcanus* at 3.7-Å resolution, Proc. Natl. Acad. Sci. U. S. A. 100 (2003) 98–103, http://dx.doi.org/10.1073/pnas.0135651100.
[8] A. Zouni, H.T. Witt, J. Kern, P. Fromme, N. Krauß, W. Saenger, P. Orth, Crystal structure of photosystem II from *Synechococcus elongatus* at 3.8 Å resolution, Nature 409 (2001) 739–743, http://dx.doi.org/10.1038/35055589.
[9] B. Hankamer, E. Morris, J. Nield, C. Gerle, J. Barber, Three-dimensional structure of the photosystem II core dimer of higher plants determined by electron microscopy, J. Struct. Biol. 135 (2001) 262–269, http://dx.doi.org/10.1006/jsbi.2001.4405.
[10] B. Hankamer, E.P. Morris, J. Barber, Revealing the structure of the oxygen-evolving core dimer of photosystem II by cryoelectron crystallography, Nat. Struct. Biol. 6 (1999) 560–564, http://dx.doi.org/10.1038/9341.
[11] K.H. Rhee, E.P. Morris, J. Barber, W. Kühlbrandt, Three-dimensional structure of the plant photosystem II reaction centre at 8 Å resolution, Nature 396 (1998) 283–286, http://dx.doi.org/10.1038/24421.
[12] M. Ballottari, J. Girardon, L. Dall'osto, R. Bassi, Evolution and functional properties of photosystem II light harvesting complexes in eukaryotes, Biochim. Biophys. Acta 1817 (2012) 143–157, http://dx.doi.org/10.1016/j.bbabio.2011.06.005.
[13] J. Standfuss, A.C.T. van Scheltinga, M. Lamborghini, W. Kühlbrandt, Mechanisms of photoprotection and nonphotochemical quenching in pea light-harvesting complex at 2.5 Å resolution, EMBO J. 24 (2005) 919–928, http://dx.doi.org/10.1038/sj.emboj.7600585.
[14] J.M. Anderson, W.S. Chow, J. De Las Rivas, Dynamic flexibility in the structure and function of photosystem II in higher plant thylakoid membranes: the grana enigma, Photosynth. Res. 98 (2008) 575–587, http://dx.doi.org/10.1007/s11120-008-9381-3.
[15] A.E. Yakushevska, P.E. Jensen, W. Keegstra, H. van Roon, H.V. Scheller, E.J. Boekema, J.P. Dekker, Supermolecular organization of photosystem II and its associated light-harvesting antenna in *Arabidopsis thaliana*, Eur. J. Biochem. 268 (2001) 6020–6028, http://dx.doi.org/10.1046/j.0014-2956.2001.02505.x.

[16] E.J. Boekema, H. van Roon, J.F. van Breemen, J.P. Dekker, Supramolecular organization of photosystem II and its light-harvesting antenna in partially solubilized photosystem II membranes, Eur. J. Biochem. 266 (1999) 444–452, http://dx.doi.org/10.1046/j.1432-1327.1999.00876.x.
[17] E.J. Boekema, H. van Roon, F. Calkoen, R. Bassi, J.P. Dekker, Multiple types of association of photosystem II and its light-harvesting antenna in partially solubilized photosystem II membranes, Biochemistry 38 (1999) 2233–2239, http://dx.doi.org/10.1021/bi9827161.
[18] E.J. Boekema, H. van Roon, J.P. Dekker, Specific association of photosystem II and light-harvesting complex II in partially solubilized photosystem II membranes, FEBS Lett. 424 (1998) 95–99, http://dx.doi.org/10.1016/S0014-5793(98)00147-1.
[19] R. Kouřil, J.P. Dekker, E.J. Boekema, Supramolecular organization of photosystem II in green plants, Biochim. Biophys. Acta 1817 (2012) 2–12, http://dx.doi.org/10.1016/j.bbabio.2011.05.024.
[20] J.P. Dekker, E.J. Boekema, Supramolecular organization of thylakoid membrane proteins in green plants, Biochim. Biophys. Acta 1706 (2005) 12–39, http://dx.doi.org/10.1016/j.bbabio.2004.09.009.
[21] H. van Amerongen, R. Croce, Light harvesting in photosystem II, Photosynth. Res. 116 (2013) 251–263, http://dx.doi.org/10.1007/s11120-013-9824-3.
[22] A.E. Yakushevska, W. Keegstra, E.J. Boekema, J.P. Dekker, J. Andersson, S. Jansson, A.V. Ruban, P. Horton, The structure of photosystem II in *Arabidopsis*: Localization of the CP26 and CP29 antenna complexes, Biochemistry 42 (2003) 608–613, http://dx.doi.org/10.1021/bi027109z.
[23] S. de Bianchi, N. Betterle, R. Kouril, S. Cazzaniga, E. Boekema, R. Bassi, L. Dall'Osto, *Arabidopsis* mutants deleted in the light-harvesting protein Lhcb4 have a disrupted photosystem II macrostructure and are defective in photoprotection, Plant Cell 23 (2011) 2659–2679, http://dx.doi.org/10.1105/tpc.111.087320.
[24] Y. Miloslavina, S. de Bianchi, L. Dall'Osto, R. Bassi, A.R. Holzwarth, Quenching in *Arabidopsis thaliana* mutants lacking monomeric antenna proteins of photosystem II, J. Biol. Chem. 286 (2011) 36830–36840, http://dx.doi.org/10.1074/jbc.M111.273227.
[25] X. Pan, M. Li, T. Wan, L. Wang, C. Jia, Z. Hou, X. Zhao, J. Zhang, W. Chang, Structural insights into energy regulation of light-harvesting complex CP29 from spinach, Nat. Struct. Mol. Biol. 18 (2011) 309–315, http://dx.doi.org/10.1038/nsmb.2008.
[26] B. van Oort, M. Alberts, S. de Bianchi, L. Dall'Osto, R. Bassi, G. Trinkunas, R. Croce, H. van Amerongen, Effect of antenna-depletion in photosystem II on excitation energy transfer in *Arabidopsis thaliana*, Biophys. J. 98 (2010) 922–931, http://dx.doi.org/10.1016/j.bpj.2009.11.012.
[27] S. de Bianchi, L. Dall'Osto, G. Tognon, T. Morosinotto, R. Bassi, Minor antenna proteins CP24 and CP26 affect the interactions between photosystem II subunits and the electron transport rate in grana membranes of *Arabidopsis*, Plant Cell 20 (2008) 1012–1028, http://dx.doi.org/10.1105/tpc.107.055749.
[28] L. Kovács, J. Damkjaer, S. Kereïche, C. Ilioaia, A.V. Ruban, E.J. Boekema, S. Jansson, P. Horton, Lack of the light-harvesting complex CP24 affects the structure and function of the grana membranes of higher plant chloroplasts, Plant Cell 18 (2006) 3106–3120, http://dx.doi.org/10.1105/tpc.106.045641.
[29] B. Drop, M. Webber-Birungi, S.K. Yadav, A. Filipowicz-Szymanska, F. Fusetti, E.J. Boekema, R. Croce, Light-harvesting complex II (LHCII) and its supramolecular organization in *Chlamydomonas reinhardtii*, Biochim. Biophys. Acta 1837 (2014) 63–72, http://dx.doi.org/10.1016/j.bbabio.2013.07.012.
[30] J. Andersson, R.G. Walters, P. Horton, S. Jansson, Antisense inhibition of the photosynthetic antenna proteins CP29 and CP26: implications for the mechanism of protective energy dissipation, Plant Cell 13 (2001) 1193–1204, http://dx.doi.org/10.1105/tpc.13.5.1193.
[31] A.V. Ruban, M. Wentworth, A.E. Yakushevska, J. Andersson, P.J. Lee, W. Keegstra, J.P. Dekker, E.J. Boekema, S. Jansson, P. Horton, Plants lacking the main light-harvesting complex retain photosystem II macro-organization, Nature 421 (2003) 648–652, http://dx.doi.org/10.1038/Nature01344.
[32] L. Dall'Osto, C. Unlu, S. Cazzaniga, H. van Amerongen, Disturbed excitation energy transfer in *Arabidopsis thaliana* mutants lacking minor antenna complexes of photosystem II, Biochim. Biophys. Acta 1837 (2014) 1981–1988, http://dx.doi.org/10.1016/j.bbabio.2014.09.011.
[33] R. Phillips, T. Ursell, P. Wiggins, P. Sens, Emerging roles for lipids in shaping membrane–protein function, Nature 459 (2009) 379–385, http://dx.doi.org/10.1038/nature08147.
[34] B. Loll, J. Kern, W. Saenger, A. Zouni, J. Biesiadka, Lipids in photosystem II: interactions with protein and cofactors, Biochim. Biophys. Acta 1767 (2007) 509–519, http://dx.doi.org/10.1016/j.bbabio.2006.12.009.
[35] J.L. Rigaud, B. Pitard, D. Levy, Reconstitution of membrane proteins into liposomes: application to energy-transducing membrane proteins, Biochim. Biophys. Acta 1231 (1995) 223–246, http://dx.doi.org/10.1016/0005-2728(95)00091-V.
[36] A.W.D. Larkum, J.M. Anderson, The reconstitution of a photosystem II protein complex, P-700-chlorophyll *a*-protein complex and light-harvesting chlorophyll *a*/*b*-protein, Biochim. Biophys. Acta 679 (1982) 410–421, http://dx.doi.org/10.1016/0005-2728(82)90162-1.
[37] D.J. Murphy, D. Crowther, I.E. Woodrow, Reconstitution of light-harvesting chlorophyll-protein complexes with photosystem II complexes in soybean phosphatidylcholine liposomes: enhancement of quantum efficiency at sub-saturating light intensities in the reconstituted liposomes, FEBS Lett. 165 (1984) 151–155, http://dx.doi.org/10.1016/0014-5793(84)80160-X.
[38] S.G. Sprague, E.L. Camm, B.R. Green, L.A. Staehelin, Reconstitution of light-harvesting complexes and photosystem II cores into galactolipid and phospholipid liposomes, J. Cell Biol. (1985) 552–557, http://dx.doi.org/10.1083/jcb.100.2.552.
[39] S.C. Darr, C.J. Arntzen, Reconstitution of the light harvesting chlorophyll *a*/*b* pigment–protein complex into developing chloroplast membranes using a dialyzable detergent, Plant Physiol. 80 (1986) 931–937, http://dx.doi.org/10.1104/pp.80.4.931.
[40] D.A. Berthold, G.T. Babcock, C.F. Yocum, A highly resolved, oxygen-evolving photosystem II preparation from spinach thylakoid membranes: EPR and electron-transport properties, FEBS Lett. 134 (1981) 231–234, http://dx.doi.org/10.1016/0014-5793(81)80608-4.
[41] R.J. Porra, W.A. Thompson, P.E. Kriedemann, Determination of accurate extinction coefficients and simultaneous equations for assaying chlorophylls *a* and *b* extracted with four different solvents: verification of concentration of chlorophyll standards by atomic absorption spectroscopy, Biochim. Biophys. Acta 975 (1989) 384–394, http://dx.doi.org/10.1016/S0005-2728(89)80347-0.
[42] B. Hankamer, J. Nield, D. Zheleva, E. Boekema, S. Jansson, J. Barber, Isolation and biochemical characterisation of monomeric and dimeric photosystem II complexes from spinach and their relevance to the organisation of photosystem II in vivo, Eur. J. Biochem. 243 (1997) 422–429, http://dx.doi.org/10.1111/j.1432-1033.1997.0422a.x.
[43] W. Rühle, H. Paulsen, Preparation of native and recombinant light-harvesting chlorophyll-*a*/*b* complex, Methods Mol. Biol. 274 (2004) 93–103, http://dx.doi.org/10.1385/1-59259-799-8:093.
[44] Z.F. Liu, H.C. Yan, K.B. Wang, T.Y. Kuang, J.P. Zhang, L.L. Gui, X.M. An, W.R. Chang, Crystal structure of spinach major light-harvesting complex at 2.72 Å resolution, Nature 428 (2004) 287–292, http://dx.doi.org/10.1038/Nature02373.
[45] C. Yang, S. Boggasch, W. Haase, H. Paulsen, Thermal stability of trimeric light-harvesting chlorophyll *a*/*b* complex (LHCIIb) in liposomes of thylakoid lipids, Biochim. Biophys. Acta 1757 (2006) 1642–1648, http://dx.doi.org/10.1016/j.bbabio.2006.08.010.
[46] H. Schägger, Tricine-SDS-PAGE, Nat. Protoc. 1 (2006) 16–22, http://dx.doi.org/10.1038/nprot.2006.4.
[47] N.J. Severs, Freeze-fracture electron microscopy, Nat. Protoc. 2 (2007) 547–576, http://dx.doi.org/10.1038/nprot.2007.55.
[48] N. Sato, M. Tsuzuki, Isolation and identification of chloroplast lipids, Methods Mol. Biol. 274 (2004) 149–157, http://dx.doi.org/10.1385/1-59259-799-8:149.
[49] A. Shevchenko, H. Tomas, J. Havliš, J.V. Olsen, M. Mann, In-gel digestion for mass spectrometric characterization of proteins and proteomes, Nat. Protoc. 1 (2006) 2856–2860, http://dx.doi.org/10.1038/nprot.2006.468.
[50] H. Xu, P.H. Hsu, L.W. Zhang, M.D. Tsai, M.A. Freitas, Database search algorithm for identification of intact cross-links in proteins and peptides using tandem mass spectrometry, J. Proteome Res. 9 (2010) 3384–3393, http://dx.doi.org/10.1021/Pr100369y.
[51] L.H. Wang, D.Q. Li, Y. Fu, H.P. Wang, J.F. Zhang, Z.F. Yuan, R.X. Sun, R. Zeng, S.M. He, W. Gao, pFind 2.0: a software package for peptide and protein identification via tandem mass spectrometry, Rapid Commun. Mass Spectrom. 21 (2007) 2985–2991, http://dx.doi.org/10.1002/rcm.3173.
[52] P.W. Hemelrijk, S.L.S. Kwa, R. van Grondelle, J.P. Dekker, Spectroscopic properties of LHC-II, the main light-harvesting chlorophyll *a*/*b* complex from chloroplast membranes, Biochim. Biophys. Acta 1098 (1992) 159–166, http://dx.doi.org/10.1016/S0005-2728(05)80331-7.
[53] E.G. Andrizhiyevskaya, A. Chojnicka, J.A. Bautista, B.A. Diner, R. van Grondelle, J.P. Dekker, Origin of the F685 and F695 fluorescence in photosystem II, Photosynth. Res. 84 (2005) 173–180, http://dx.doi.org/10.1007/s11120-005-0478-7.
[54] T.P. Krüger, C. Ilioaia, M.P. Johnson, A.V. Ruban, R. van Grondelle, Disentangling the low-energy states of the major light-harvesting complex of plants and their role in photoprotection, Biochim. Biophys. Acta 1837 (2014) 1027–1038, http://dx.doi.org/10.1016/j.bbabio.2014.02.014.
[55] A. Andreeva, K. Stoitchkova, M. Busheva, E. Apostolova, Changes in the energy distribution between chlorophyll–protein complexes of thylakoid membranes from pea mutants with modified pigment content. I. Changes due to the modified pigment content, J. Photochem. Photobiol. B 70 (2003) 153–162, http://dx.doi.org/10.1016/S1011-1344(03)00075-7.
[56] S. Malkin, P.A. Armond, H.A. Mooney, D.C. Fork, Photosystem II photosynthetic unit sizes from fluorescence induction in leaves: correlation to photosynthetic capacity, Plant Physiol. 67 (1981) 570–579, http://dx.doi.org/10.1104/pp.67.3.570.
[57] G. Bonente, S. Pippa, S. Castellano, R. Bassi, M. Ballottari, Acclimation of *Chlamydomonas reinhardtii* to different growth irradiances, J. Biol. Chem. 287 (2012) 5833–5847, http://dx.doi.org/10.1074/jbc.M111.304279.
[58] S. Haferkamp, W. Haase, A.A. Pascal, H. van Amerongen, H. Kirchhoff, Efficient light harvesting by photosystem II requires an optimized protein packing density in grana thylakoids, J. Biol. Chem. 285 (2010) 17020–17028, http://dx.doi.org/10.1074/jbc.M109.077750.
[59] F. Zhou, S. Liu, Z. Hu, T. Kuang, H. Paulsen, C. Yang, Effect of monogalactosyldiacylglycerol on the interaction between photosystem II core complex and its antenna complexes in liposomes of thylakoid lipids, Photosynth. Res. 99 (2009) 185–193, http://dx.doi.org/10.1007/s11120-008-9388-9.
[60] O.S. Andersen, R.E. Koeppe, Bilayer thickness and membrane protein function: an energetic perspective, Annu. Rev. Biophys. Biomol. Struct. 36 (2007) 107–130, http://dx.doi.org/10.1146/annurev.biophys.36.040306.132643.
[61] B. de Kruijff, Lipid polymorphism and biomembrane function, Curr. Opin. Chem. Biol. 1 (1997) 564–569, http://dx.doi.org/10.1016/S1367-5931(97)80053-1.
[62] H. Liu, H. Zhang, D.M. Niedzwiedzki, M. Prado, G. He, M.L. Gross, R.E. Blankenship, Phycobilisomes supply excitations to both photosystems in a megacomplex in cyanobacteria, Science 342 (2013) 1104–1107, http://dx.doi.org/10.1126/science.1242321.
[63] S. Caffarri, R. Kouřil, S. Kereïche, E.J. Boekema, R. Croce, Functional architecture of higher plant photosystem II supercomplexes, EMBO J. 28 (2009) 3052–3063, http://dx.doi.org/10.1038/emboj.2009.232.
[64] L. Wilk, M. Grunwald, P.N. Liao, P.J. Walla, W. Kühlbrandt, Direct interaction of the major light-harvesting complex II and PsbS in nonphotochemical quenching, Proc. Natl. Acad. Sci. U. S. A. 110 (2013) 5452–5456, http://dx.doi.org/10.1073/pnas.1205561110.

[65] J. Nield, J. Barber, Refinement of the structural model for the photosystem II supercomplex of higher plants, Biochim. Biophys. Acta 1757 (2006) 353–361, http://dx.doi.org/10.1016/j.bbabio.2006.03.019.
[66] R. Remelli, C. Varotto, D. Sandonà, R. Croce, R. Bassi, Chlorophyll binding to monomeric light-harvesting complex. A mutation analysis of chromophore-binding residues, J. Biol. Chem. 274 (1999) 33510–33521, http://dx.doi.org/10.1074/jbc.274.47.33510.
[67] V.I. Novoderezhkin, M.A. Palacios, H. van Amerongen, R. van Grondelle, Excitation dynamics in the LHCII complex of higher plants: modeling based on the 2.72 Å crystal structure, J. Phys. Chem. B 109 (2005) 10493–10504, http://dx.doi.org/10.1021/jp044082f.
[68] R.C. Jennings, F.M. Garlaschi, L. Finzi, G. Zucchelli, Slow exciton trapping in photosystem II: a possible physiological role, Photosynth. Res. 47 (1996) 167–173, http://dx.doi.org/10.1007/Bf00016179.
[69] R. Croce, H. van Amerongen, Light-harvesting and structural organization of photosystem II: from individual complexes to thylakoid membrane, J. Photochem. Photobiol. B 104 (2011) 142–153, http://dx.doi.org/10.1016/j.jphotobiol.2011.02.015.
[70] F. Muh, C. Glockner, J. Hellmich, A. Zouni, Light-induced quinone reduction in photosystem II, Biochim. Biophys. Acta 1817 (2012) 44–65, http://dx.doi.org/10.1016/j.bbabio.2011.05.021.